Jan Verspecht bvba

Mechelstraat 17
B-1745 Opwijk
Belgium

email: contact@janverspecht.com
web: http://www.janverspecht.com

Extension of X-parameters to Include Long-Term Dynamic Memory Effects

Jan Verspecht, Jason Horn, Loren Betts, Daniel Gunyan, Roger Pollard, Chad Giillease, David E. Root

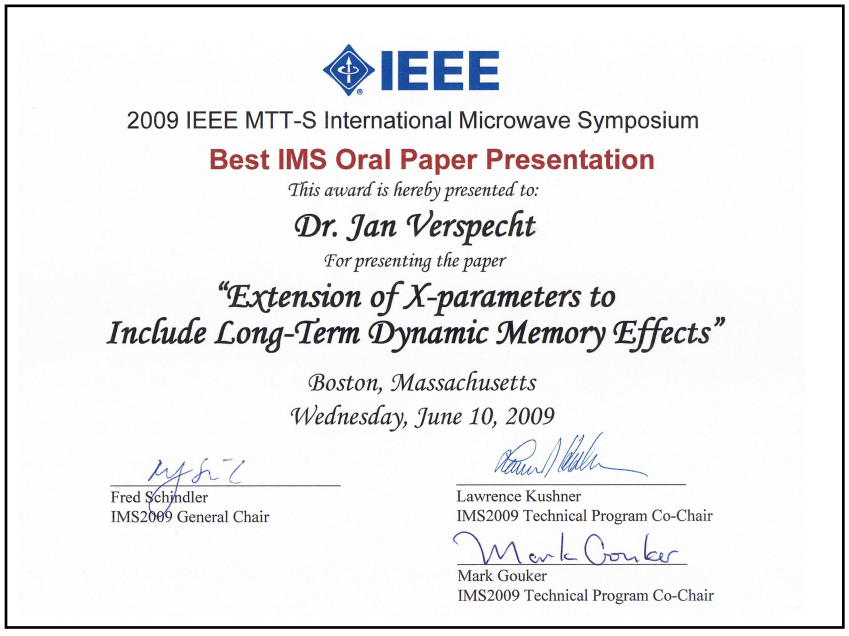

Presented at the 2009 International Microwave Symposium - Boston, USA

Extension of X-parameters to Include Long-Term Dynamic Memory Effects

Jan Verspecht*, Jason Horn**, Loren Betts**, Daniel Gunyan**, Roger Pollard***, Chad Gillease**, and David E. Root**

* Jan Verspecht b.v.b.a., Opwijk, Vlaams-Brabant, B-1745, Belgium
** Agilent Technologies, Inc., Santa Rosa, California, CA 95403, USA
*** University of Leeds, Leeds, LS2 9JT, United Kingdom

***Abstract*—A new unified theory and methodology is presented to characterize and model long-term memory effects of microwave components by extending the Poly-Harmonic Distortion (PHD) Model to include dynamics that are identified from pulsed envelope X-parameter measurements on an NVNA. The model correctly predicts the transient RF response to time-varying RF excitations including the asymmetry between off-to-on and on-to-off switched behavior as well as responses to conventional wide-bandwidth communication signals that excite long-term memory effects in power amplifiers. The model is implemented in the ADS circuit envelope simulator.**

***Index Terms*—behavioral model, memory effects, frequency domain, measurements, X-parameters, NVNA, PHD model**

I. Introduction

Behavioral modeling of microwave components is of great interest to the designers of amplifiers that are used in today's wireless communication infrastructure. An important problem faced by these engineers is the difficulty to characterize, describe mathematically, and simulate the nonlinear behavior of amplifiers that are stimulated by signals that have a high peak-to-average ratio and that excite the amplifier over the full operating range of instantaneous power. This is problematic for at least two reasons. Firstly, the amplifier behavior may be driven into full saturation and is as such strongly nonlinear. Secondly, the amplifier behavior shows long-term memory effects. Such memory effects are caused, among others, by time-varying operating conditions such as dynamic self-heating and bias-line modulation. These changes are induced by the input signal itself and vary at a relatively slow rate compared to the modulation speed. As a consequence the instantaneous behavior of the amplifier becomes a function not only of the instantaneous value of the input signal, but also of the past values of the input signal. This is referred to as a "long term memory effect".

In this paper we develop an original behavioral model that can handle both strongly nonlinear effects and long-term dynamic memory effects. One of the advantages of the new approach is that the model can be extracted by performing a set of pulsed envelope X-parameter measurements on a modern Nonlinear Vector Network Analyzer (NVNA). Another advantage is that the model remains valid for a wide range of modulation bandwidths, which is typically not the case for classic approaches.

II. Model Theory

As described in [2] memory effects can be introduced by making use of one or more hidden variables. The idea is that, in a system with memory, the mapping from the input signal to the output signal is no longer a function of the input signal amplitude only, but is also a function of an arbitrary number N of *a priori* unknown hidden variables, denoted $h_1(t)$, $h_2(t),\ldots,h_N(t)$. These variables represent time varying physical quantities inside the component, for example temperature, bias voltages or currents, or semiconductor trapping phenomena that influence the mapping from the input RF signal to the output signal. For simplicity we deal with a unilateral and perfectly matched device and neglect all harmonics. Extensions to multi-port devices with mismatch and harmonics will be treated elsewhere.

The time-dependent envelope of the scattered wave B(t) is given by a generic nonlinear function F(.) of the input amplitude envelope A(t) and the time-dependent values of all relevant hidden state variables, $h_i(t)$, as described by (1).

$$B(t) = F\left(\left|A(t)\right|, h_1(t), h_2(t), ..., h_N(t)\right).\Phi(t) \tag{1}$$

For simplified notation in (1) we define $\Phi(t) = e^{j\phi(A(t))}$

The work of [2] showed the dependence of B(t) on the phase of A(t) modeled by (1) is a good approximation for many systems and its limitation will not be considered further here.

The black-box assumption about the relationship between the input signal A(t) and the hidden variables $h_i(t)$ is

mathematically expressed as

$$h_i(t) = \int_0^\infty P_i\left(\left|A(t-u)\right|\right) k_i(u)\,du\,. \quad (2)$$

Equation (2) expresses that the i^{th} hidden variable is generated by a linear filter operation, characterized by its impulse response $k_i(.)$, that operates on a nonlinear function $P_i(.)$ of the input signal amplitude $|A(.)|$. $P_i(.)$ can be interpreted as a source term that describes how the input signal is related to the excitation of a particular hidden variable. For example, $P_i(.)$ could describe the power dissipation as a function of the input signal amplitude, whereby $h_i(.)$ is the temperature. The impulse response $k_i(.)$ describes the actual dynamics of a hidden variable, e.g. the thermal relaxation. Note that the model as described in [2] is actually a special case of (1) and (2).

To derive an easily identifiable model, we choose to linearize (1) around the deviation between the steady state solution for the hidden variables at fixed RF amplitude, and their instantaneous values due to the actual time-varying input envelope. After some algebra, the resulting approximation to (1) becomes

$$B(t) = \left(F_{CW}\left(\left|A(t)\right|\right) + \int_0^\infty G\left(\left|A(t)\right|, \left|A(t-u)\right|, u\right)du\right)\Phi(t) \quad (3)$$

where

$$F_{CW}\left(\left|A(t)\right|\right) = F\left(\left|A(t)\right|, h_1\left(\left|A(t)\right|\right), h_2\left(\left|A(t)\right|\right), ...\right) \quad (4)$$

$$h_i(A(t)) = P_i\left(\left|A(t)\right|\right)\int_0^\infty k_i(u)\,du \quad (5)$$

$$G(x,y,u) = \sum_{i=1}^{N} D_i(x)\left(P_i(y) - P_i(x)\right)k_i(u) \quad (6)$$

and $$D_i(x) = \left.\frac{\partial F}{\partial h_i}\right|_{(x,h_1(x),h_2(x)...)}\,. \quad (7)$$

Note $F_{cw}(.)$ is defined by the value of F when, at each time, t, the hidden variables take the values they would have achieved under a steady-state condition corresponding to an amplitude A(t).

III. Model Identification

$F_{cw}(.)$ is nothing more than the conventional static PHD model (neglecting mismatch and harmonics) and can therefore be identified by conventional CW X-parameters [1,9]. The remaining term in (3) contains the memory effects, written as the integral of a nonlinear function of the instantaneous signal amplitude and all prior values of the signal amplitude.

By evaluating (3) for a stepped input envelope amplitude starting from A_1 at t<0 to A_2 at t>=0, one derives from (3) and the properties of (6) the following relationship between the corresponding transient envelope response B(t) and the memory kernel G(x,y,u) given by (8).

$$G\left(\left|A_2\right|, \left|A_1\right|, t\right) = -\frac{dB(t)}{dt}.\exp\left(-j\varphi\left(A_2\right)\right) \quad (8)$$

Equation 8 demonstrates G(x,y,t) can be determined from the set of time-dependent step responses from all initial values y to all final values x.

There is a one-to-one mapping between the model and the step responses, so this model will perfectly predict the detailed time-dependence of the step responses from any initial input envelope amplitude to any other. No other model known to the authors has this capability.

IV. Experimental Results

The theory described above is experimentally validated on two nonlinear components, a single on-wafer bare HBT transistor and an Anadigics AWT6282 linear power amplifier module. There are two steps to the process, model extraction and model validation. An Agilent NVNA [10] is used for the measurement of the set of pulsed A(t) and B(t) complex waveforms, using the technique described in [8].

A. Model Extraction

For the model extraction a set of pulsed envelope X-parameter measurements is performed covering the complete range of input amplitudes from zero to the maximum possible amplitude. For the transistor measurements, a set of 20 different values are chosen for the initial and final input amplitudes, A_1 and A_2, ranging from small signal excitations to fully saturating excitations. This results in a total of 400 possible amplitude transitions. For each large signal input step A(t), the corresponding B(t) step response is sampled. When performing the measurements, the sampling window B(t) is chosen large enough to ensure that B(t) has reached its steady state at the last sample. For the experiment a total of 3000 time samples were measured for B(t) using a sampling time of 50ns, which results in a total sampling window of 150us. Fig.1 and Fig.2 depict the amplitudes of two such large signal step responses, selected among the total of 400 measurements. Fig.1 corresponds to A(t) (red) and B(t) (blue) with a transition at the input from 0.1V (-10dBm) to 0.5V (4dBm), and Fig.2 corresponds to the inverse step whereby the input signal switches from 0.5V (4dBm) to 0.1V (-10dBm). Note that not only the amplitude of B(t) is measured, but also the phase. Fig.3 depicts both of the measured phases of B(t) for the abovementioned transitions. The phase corresponding to the transition from low to high is depicted in red; the phase of the transition from high to low is depicted in blue.

Next, the measured data is processed in order to extract the model functions $F_{CW}(.)$ and $G(.)$. First $F_{CW}(.)$ is determined by simply using the last samples of the measured B(t) step responses. It is hereby assumed that steady state has been reached for the last B(t) sample. The value of $G(.)$ is determined by calculating the time derivative of the measured large signal step responses, as described by (8).

Fig.4 depicts the amplitude of the measured 3-variate kernel $G(.)$ with the third argument (time "t") constant and equal to 5us. The x-axis (indicated on the left) represents the first argument of $G(.)$, namely A_2 (amplitude after the step), the y-axis (indicated on the right) represents the second argument A_1. The amplitude of $G(.)$ is represented on the z-axis. Note that the unit of $G(.)$ is Volt per second. The high amplitude of $G(.)$ for A_1 equal to 0.2V and for A_2 equal to 0.4V can, for example, be interpreted as follows: an input amplitude of 0.4V induces a significant memory effect which, after 5us, shows up prominently at an instantaneous amplitude of 0.2V.

The same procedure is applied to the PA module. For this example, the maximum amplitude for the steps is 0.63V, and there are 8000 time samples at 50ns time-steps.

B. Model Validation

The model validation is done by performing 2-tone measurements with varying input amplitude and frequency offsets. The validation measurements are also performed by using the NVNA in envelope mode.

Once $F_{CW}(.)$ and $G(.)$ have been identified, the model described by (3) is implemented in the envelope simulator of ADS. During the simulation the measured input envelopes A(t) corresponding to a two-tone sinusoidal signal are applied to the input of the model and the simulator calculates the corresponding output envelopes, $B_{SIM}(t)$. Validation results are shown only for the PA module.

The instantaneous linear gain of the PA module is plotted versus the peak input envelope amplitude in Volts in Fig. 5, of a two-tone input at a frequency difference of 19.2 kHz centered at 1.75GHz with equal tone powers of 1dBm. The significant looping of the measured characteristics (red), a signature of memory effects, is well approximated by the model predictions in simulation (blue). The static model simulation, obtained by including only the first term in (3), is shown in black.

The simulated and measured time-dependent output envelopes are compared in Fig 6 as a function of time over a period of about 11 us centered around the peak of the time-varying envelope response. These results correspond to a frequency difference of 38.4 kHz also centered at 1.75GHz. The measured output envelope B(t) is represented in red and the simulated output envelope, $B_{SIM}(t)$, is represented in blue, The traces are nearly coincident. The magenta curve represents the results of using the static model. The measured B(t) and modeled $B_{SIM}(t)$ show a significant memory effect since the falling envelopes are considerably lower than the corresponding values during the rise, despite the fact that the input envelope is symmetric.

Another manifestation of memory effects is the tone-spacing dependence of intermodulation spectra. Fig. 7 shows measured (red) and modeled (blue) IM3 results of the PA module by varying the input tone spacing from 9600Hz to 6.25MHz. The model is able to capture the offset-frequency dependence over this wide frequency range, including the sharp resonances.

V. CONCLUSIONS

A new unified approach to the characterization, modeling, and simulation of dynamic long-tern memory has been presented. Memory effects have been identified from pulsed envelope transient X-parameter measurements on an NVNA. A powerful theory has been developed to relate this data to a nonlinear dynamical model. Together, the approach extends the X-parameter paradigm and PHD model to long-term dynamic memory effects such as self-heating, dynamic bias effects, and trapping phenomena. The approach has been applied to an HBT transistor and a commercial PA module that exhibit significant memory effects. The resulting memory model has been experimentally validated by two-tone NVNA measurements using novel envelope transient measurement techniques. The model offers significant advantages compared to previous approaches in the literature in that it correctly models both turn-on and turn-off transient effects as well as provides a dynamic model sufficiently accurate for wide band-width communication signals with high peak-to-average ratios.

REFERENCES

[1] J. Verspecht and D. Root, "Polyharmonic Distortion Modeling," *IEEE Microwave Magazine*, vol. 7, no. 3, pp. 44-57, June 2006.

[2] J. Verspecht et al., "Multi-port, and Dynamic Memory Enhancements to PHD Nonlinear Behavioral Models from Large-signal Measurements and Simulations", *Conference Record of the IEEE Microwave Theory and Techniques Symposium 2007*, pp.969-972, USA, June 2007.

[3] J. C. Pedro et al., "A Comparative Overview of Microwave and Wireless Power-Amplifier Behavioral Modeling Approaches," *IEEE Transactions on Microwave Theory and Techniques*, Vol.53, No.4, April 2005.

[4] F. Filicori et al., "A Nonlinear Integral Model of Electron Devices for HB Circuit Analysis," *IEEE Transactions on Microwave Theory and Techniques*, Vol. 40, No. 7, pp. 1456-1465, July 1992.

[5] A. Soury et al.,"A New Behavioral Model taking into account Nonlinear Memory Effects and Transient Behaviors in Wideband SSPAs," *2002 IEEE MTT-S Conference Digest*, pp. 853-856, June 2002.

[6] J. Wood and D. E. Root,"Fundamentals of Nonlinear Behavioral Modeling for RF and Microwave Design," Chap 3, Artech House, 2005.

[7] M. Isaksson et al.,"A Comparative Analysis of Behavioral Models for RF Power Amplifiers," *IEEE Transactions on Microwave Theory and Techniques*, Vol. 54, No. 1, pp. 348-359, January 2006.

[8] Loren Betts, "Vector and Harmonic Amplitude/Phase Corrected Multi-Envelope Stimulus Response Measurements of Nonlinear Devices," *IEEE MTT-S Internatonal Microwave Symposium 2008* , pp. 261-264

[9] D. E. Root, J. Verspecht, D. Sharrit, J. Wood, and A. Cognata, **"**Broad-Band, Poly-Harmonic Distortion (PHD) Behavioral Models from Fast Automated Simulations and Large-Signal Vectorial Network Measurements," *IEEE Transactions on Microwave Theory and* Techniques Vol. 53. No. 11, November, 2005 pp. 3656-3664

[10] http://www.agilent.com/find/nvna

[11] A. Soury and E. Ngoya, "A Two-Kernel Nonlinear Impulse Response Model for Handling Long Term Memory Effects in RF and Microwave Solid State Circuits," *IEEE MTT-S International Microwave Symposium Digest*, June 2006 pp:1105 - 1108

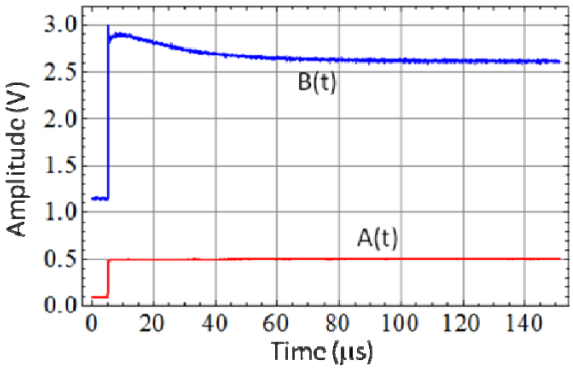

Fig. 1. Measured low-to-high large-signal step response magnitude

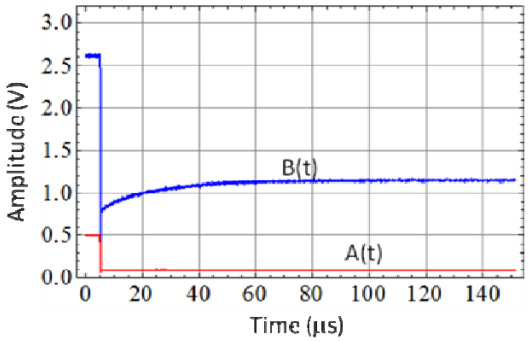

Fig. 2. Measured high-to-low large-signal step response magnitude

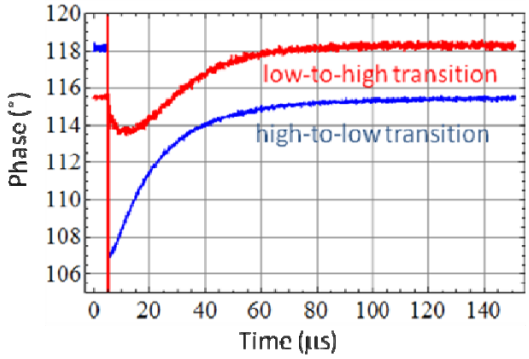

Fig. 3. Phase of the measured large signal step responses

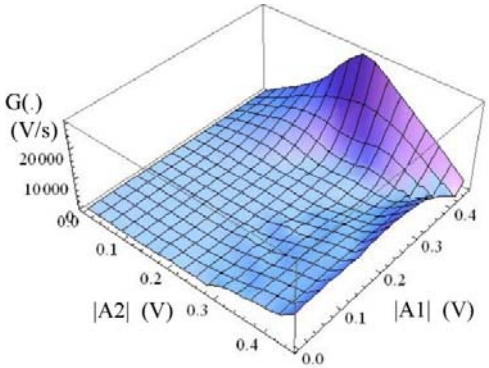

Fig. 4 Magnitude of extracted $G(A_1, A_2, t)$ for t = 5 µs

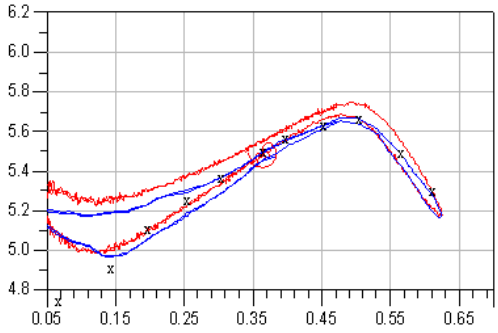

Fig. 5 Measured (red) and modeled (blue) amplifier linear instantaneous gain vs peak input voltage at 19.2kHz tone spacing. Static prediction (black Xs).

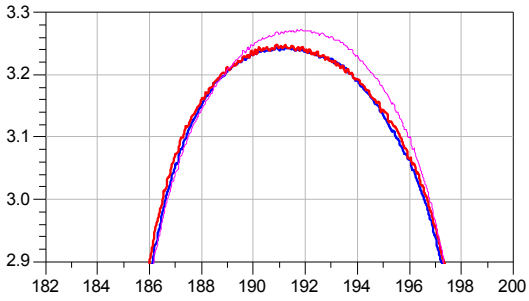

Fig. 6 Measured (red) and simulated model (blue) envelope waveforms vs time [us] for two-tone response at 1dBm tone powers, 38.4kHz spacing. Simulated (magenta) with static model.

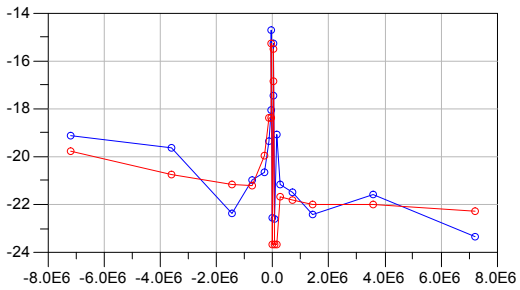

Fig. 7 Measured (red) versus model (blue) IM3 [dBm] for different tone spacings.